NASA/TM-20230001718 AIAA 2023-1750

Control Architecture for a Concept Aircraft With a Series/Parallel Partial Hybrid Powertrain and Distributed Electric Propulsion

Jonathan S. Litt, Jonathan L. Kratz, Santino J. Bianco, Jonah J. Sachs-Wetstone, and Timothy P. Dever
Glenn Research Center, Cleveland, Ohio

Halle E. Buescher
HX5, LLC, Brook Park, Ohio

Nicholas C. Ogden, Felipe D. Valdez, Daniel W. Budolak, and Matthew J. Boucher
Armstrong Flight Research Center, Edwards, California

Andrew P. Patterson
Langley Research Center, Hampton, Virginia

Ralph H. Jansen
Glenn Research Center, Cleveland, Ohio

February 2023

NASA STI Program . . . in Profile

Since its founding, NASA has been dedicated to the advancement of aeronautics and space science. The NASA Scientific and Technical Information (STI) Program plays a key part in helping NASA maintain this important role.

The NASA STI Program operates under the auspices of the Agency Chief Information Officer. It collects, organizes, provides for archiving, and disseminates NASA's STI. The NASA STI Program provides access to the NASA Technical Report Server—Registered (NTRS Reg) and NASA Technical Report Server—Public (NTRS) thus providing one of the largest collections of aeronautical and space science STI in the world. Results are published in both non-NASA channels and by NASA in the NASA STI Report Series, which includes the following report types:

- TECHNICAL PUBLICATION. Reports of completed research or a major significant phase of research that present the results of NASA programs and include extensive data or theoretical analysis. Includes compilations of significant scientific and technical data and information deemed to be of continuing reference value. NASA counter-part of peer-reviewed formal professional papers, but has less stringent limitations on manuscript length and extent of graphic presentations.

- TECHNICAL MEMORANDUM. Scientific and technical findings that are preliminary or of specialized interest, e.g., "quick-release" reports, working papers, and bibliographies that contain minimal annotation. Does not contain extensive analysis.

- CONTRACTOR REPORT. Scientific and technical findings by NASA-sponsored contractors and grantees.

- CONFERENCE PUBLICATION. Collected papers from scientific and technical conferences, symposia, seminars, or other meetings sponsored or co-sponsored by NASA.

- SPECIAL PUBLICATION. Scientific, technical, or historical information from NASA programs, projects, and missions, often concerned with subjects having substantial public interest.

- TECHNICAL TRANSLATION. English-language translations of foreign scientific and technical material pertinent to NASA's mission.

For more information about the NASA STI program, see the following:

- Access the NASA STI program home page at http://www.sti.nasa.gov

- E-mail your question to help@sti.nasa.gov

- Fax your question to the NASA STI Information Desk at 757-864-6500

- Telephone the NASA STI Information Desk at 757-864-9658

- Write to:
  NASA STI Program
  Mail Stop 148
  NASA Langley Research Center
  Hampton, VA 23681-2199

NASA/TM-20230001718 AIAA 2023-1750

Control Architecture for a Concept Aircraft With a Series/Parallel Partial Hybrid Powertrain and Distributed Electric Propulsion

Jonathan S. Litt, Jonathan L. Kratz, Santino J. Bianco, Jonah J. Sachs-Wetstone, and Timothy P. Dever
Glenn Research Center, Cleveland, Ohio

Halle E. Buescher
HX5, LLC, Brook Park, Ohio

Nicholas C. Ogden, Felipe D. Valdez, Daniel W. Budolak, and Matthew J. Boucher
Armstrong Flight Research Center, Edwards, California

Andrew P. Patterson
Langley Research Center, Hampton, Virginia

Ralph H. Jansen
Glenn Research Center, Cleveland, Ohio

Prepared for the
AIAA SciTech Forum
sponsored by the American Institute of Aeronautics and Astronautics
National Harbor, Maryland, January 23–27, 2023

National Aeronautics and
Space Administration

Glenn Research Center
Cleveland, Ohio 44135

February 2023

Acknowledgments

The Convergent Aeronautics Solutions Project sponsors this work with the support of the Transformational Tools and Technologies Project, both of which are part of the Transformative Aeronautics Concepts Program in the NASA Aeronautics Research Mission Directorate.

This work was sponsored by the
Transformative Aeronautics Concepts Program.

Level of Review: This material has been technically reviewed by technical management.

This report is available in electronic form at https://www.sti.nasa.gov/ and https://ntrs.nasa.gov/

Control Architecture for a Concept Aircraft With a Series/Parallel Partial Hybrid Powertrain and Distributed Electric Propulsion

Jonathan S. Litt, Jonathan L. Kratz, Santino J. Bianco, Jonah J. Sachs-Wetstone, and Timothy P. Dever
National Aeronautics and Space Administration
Glenn Research Center
Cleveland, Ohio 44135

Halle E. Buescher
HX5, LLC
Brook Park, Ohio 44142

Nicholas C. Ogden, Felipe D. Valdez, Daniel W. Budolak, and Matthew J. Boucher
National Aeronautics and Space Administration
Armstrong Flight Research Center
Edwards, California 93523

Andrew P. Patterson
National Aeronautics and Space Administration
Langley Research Center
Hampton, Virginia 23681

Ralph H. Jansen
National Aeronautics and Space Administration
Glenn Research Center
Cleveland, Ohio 44135

Abstract

Traditional aircraft propulsion control approaches are insufficient for electrified aircraft powertrains due to their increased complexity compared to current systems. New control approaches are required to manage the increased interdependency and complexity of these electrified powertrains. Additionally, electrification enables aircraft to have multiple distributed thrust producing fans that the flight control system can leverage for enhanced maneuverability, further increasing the control complexity. This paper describes the control architecture for a concept vehicle with these characteristics, the SUbsonic Single Aft eNgine (SUSAN) Electrofan. SUSAN is a series/parallel partial hybrid electric single-aisle transport aircraft that leverages its electrified powertrain to provide fuel burn and emissions benefits when compared to the state-of-the-art. Achieving these benefits requires an appropriately designed control architecture that coordinates the various powertrain and flight control subsystems. As such, the SUSAN aircraft is designed with a high level of automation, allowing it to properly manage coupled subsystems and react rapidly to failures and anomalies. This paper presents a summary of the SUSAN powertrain design and discusses several of the novel control approaches used to manage the complex electrified powertrain.

Nomenclature

AC	Alternating Current
AGTF30	Advanced Geared Turbofan 30K
BLI	Boundary Layer Ingesting
BMS	Battery Management System
DC	Direct Current
DEP	Distributed Electric Propulsion
EAP	Electrified Aircraft Propulsion
EE	Electric Engine
EM	Electric Machine
ESD	Energy Storage Device
GTE	Gas Turbine Engine
h	Altitude
HPC	High-Pressure Compressor
HPS	High-Pressure Spool
HPT	High-Pressure Turbine
i	current
IFPC	Integrated Flight and Propulsion Control
IVHM	Integrated Vehicle Health Management
LPC	Low-Pressure Compressor
LPS	Low-Pressure Spool
LPT	Low-Pressure Turbine
MN	Mach Number
N2	HPS Speed
Nf	Fan Speed
Nfc	Corrected Fan Speed
NPSS	Numerical Propulsion System Simulation
PI	Proportional-Integral
PID	Proportional-Integral-Derivative
PLA	Power Lever Angle
PR	Pressure Ratio
Ps3	Compressor Exit Static Pressure
Q_{max}	Maximum Battery SOC
Q_{min}	Minimum Battery SOC
SOC	State of Charge
SUSAN	SUbsonic Single Aft eNgine (SUSAN)
T	Thrust Command
T45	Turbine Exit Temperature
TEEM	Turbine Electrified Energy Management
V	Airspeed
VAFN	Variable Area Fan Nozzle
VBV	Variable Bleed Valve
V_{max}	Maximum Battery Voltage
V_{min}	Minimum Battery Voltage
VSV	Variable Stator Vanes
Wc	corrected flow

Wf	Fuel Flow Rate
X	State Vector
δ	Control effector vector
γ	Flight Path Angle
σ	Course Angle
τ_c	torque command
ω	motor speed
ω_c	motor speed command
(ϕ,θ,ψ)	Vehicle Orientation (roll, pitch, yaw)
(p,q,r)	Body Frame Rotational Rates about the body frame x, y, and z axes, respectively

Introduction

The SUbsonic Single Aft eNgine (SUSAN) Electrofan (Figure 1) is a subsonic regional jet transport aircraft concept that utilizes electrified aircraft propulsion (EAP) to enable propulsive and aerodynamic benefits to reduce fuel usage, emissions, and cost. The target market is the regional low-cost carrier airline with mission specification: 180 passengers, design range of 2500 miles, economic range of 750 miles, speed of Mach 0.78 (Ref. 1). The details of the concept are evolving, but the consistent features include a single boundary layer-ingesting (BLI) turbofan gas turbine engine (GTE) with generators driving a series/parallel partial hybrid EAP system (Figure 2). The current iteration of SUSAN has 16 underwing contrarotating BLI fans (electric engines or EEs), eight on each side.[1] Generally, a single GTE would present a certification problem as an engine failure could prove catastrophic. The SUSAN concept attempts to overcome this by using single-use (primary) batteries to provide emergency power to the EEs in case of GTE or generator failure. Relatively small reusable (secondary) batteries are also present to enable various EAP benefits. A diagram of the powertrain is shown in Figure 3 (Ref. 2). To fully achieve the potential benefits of the design, a control system needs to coordinate the operation of the subsystems. This paper discusses the control architecture and how the pieces work together to optimize the performance of this highly integrated vehicle design.

The rest of this paper is organized as follows. The powertrain is described, and the overall control concept is presented. This is followed by more detailed descriptions of the various individual control systems, and their structure and interactions are discussed. Finally, a discussion and summary are presented.

Figure 1.—Rendering of current version SUSAN concept aircraft.

[1]Note that for this paper, Electric Engine is used to mean the entire contrarotating BLI fan.

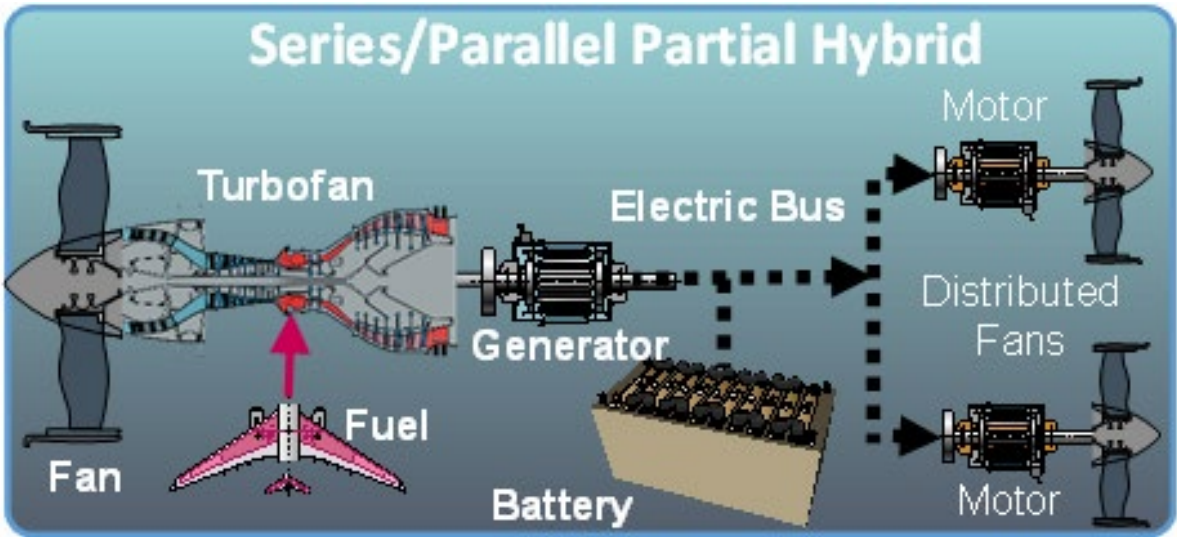

Figure 2.—Series/parallel partial hybrid EAP architecture.

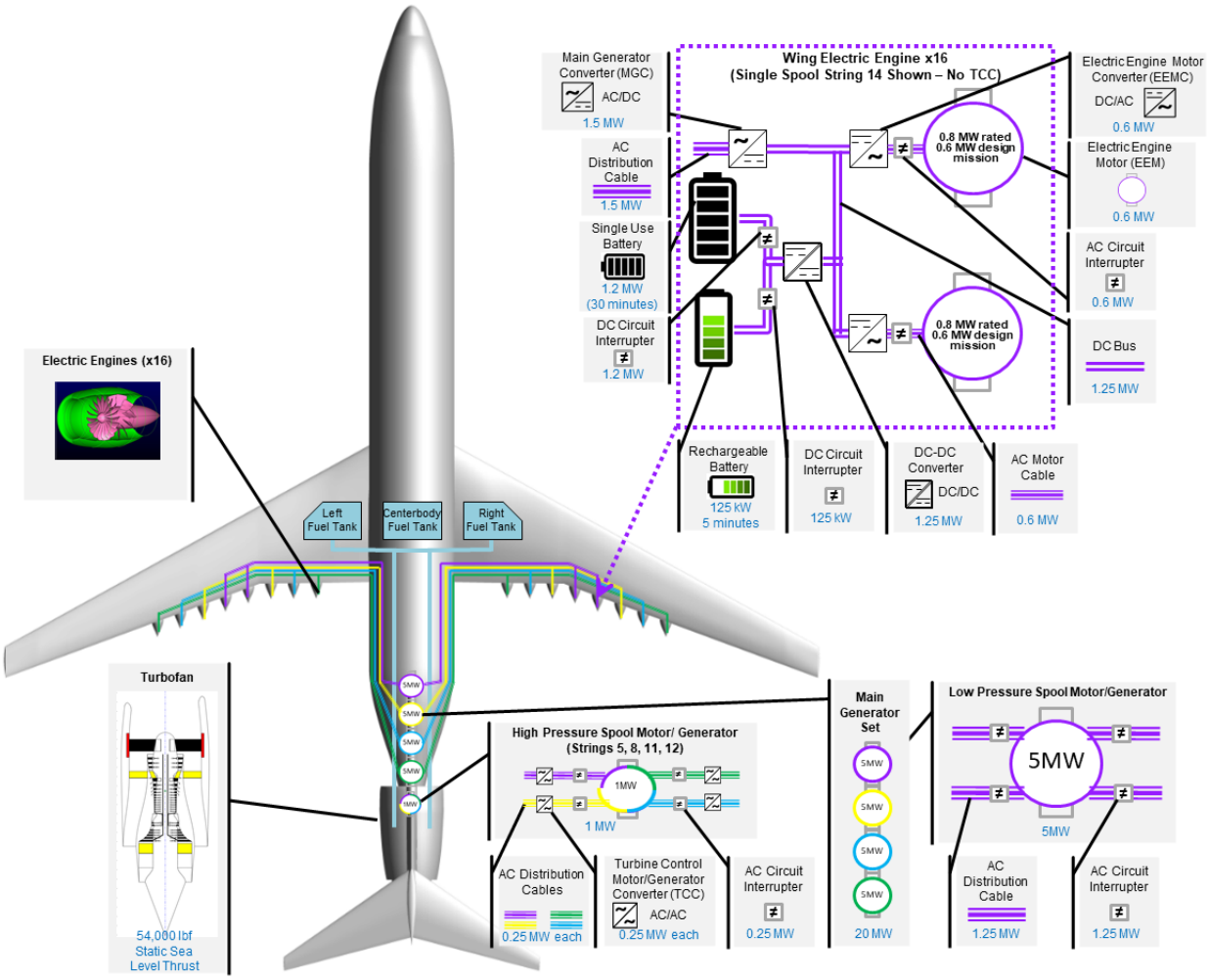

Figure 3.—Diagram of the SUSAN powertrain.

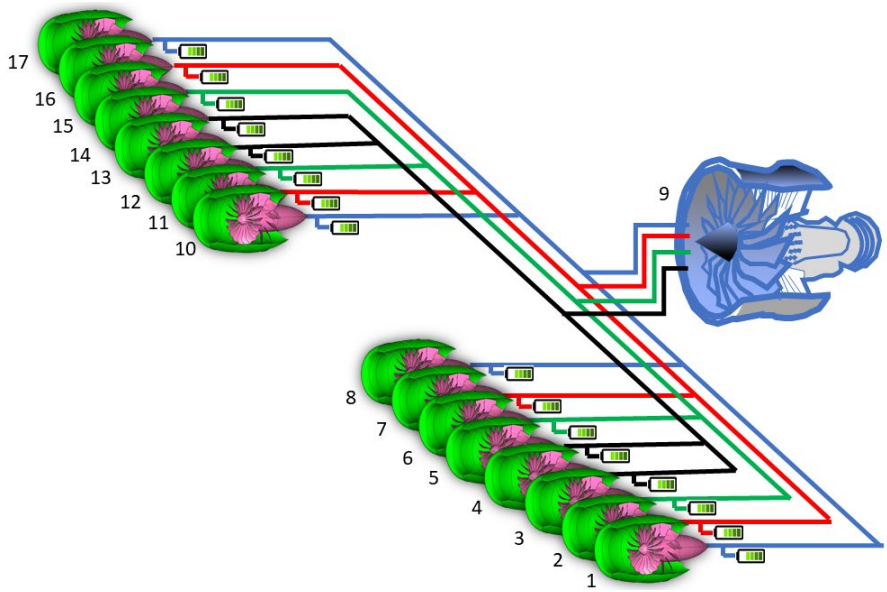

Figure 4.—SUSAN powertrain showing engine numbering.

Powertrain Design

The fully integrated nature of the SUSAN vehicle makes the powertrain functionality central to the control design effort. As shown in Figure 3, the powertrain in its current configuration includes a single BLI GTE in the tail. Power is extracted from it through four 5 MW motor/generators (electric machines or EMs) connected to the Low-Pressure Spool (LPS) and a single 1 MW EM on the High-Pressure Spool (HPS). These generators are connected to buses that distribute power to operate the 16 EEs under the wings. The engines are numbered 1-17 from left to right from the pilot's point of view, with the centrally located GTE identified as number 9. Four three-phase power buses from each of the 5 MW main generators connect to four EEs symmetrically across the wings (1, 8, 10, 17), (2, 7, 11,16), (3, 6, 12,15), and (4, 5, 13, 14), as shown in Figure 4. This ensures that a generator failure will not result in a thrust asymmetry. The 1 MW generator also has four three-phase power buses, one each attached to a single EE tied to each of the main generators (5, 8, 11, 12) (not shown in Figure 4). Although four buses share each generator, the power for each bus is demanded independently up to its current limit or the total power limit of the generator. The components are designed such that throughout the flight envelope, the thrust is split 1/3 from the GTE and 2/3 from the EEs in total, which requires a large amount of power extraction. A small rechargeable battery is attached to each bus through a DC-DC converter. This battery has multiple functions related to control and operation of the aircraft, including, providing a boost capability during climb, enabling rapid acceleration of the EEs, facilitating GTE operability improvements, and helping to maintain bus voltage.

Control System Overview

Unlike a traditional multiengine aircraft in which pilots have individual throttles they can manipulate independently, the SUSAN powertrain operation is complex, and no pilot intervention is permitted beyond the movement of a single throttle (Ref. 3).[2] Furthermore, the distributed propulsion provides enhanced maneuverability that the flight control system can leverage. These interactions require the

[2]Based on the current concept of nominal operation, but this is an area of on-going research.

control system to coordinate multiple subsystems simultaneously, respecting the constraints of each. An advantage of this, indeed one that helps to optimize the overall vehicle, is that the design relies on the ability of the control system to facilitate the interactions. This coordination optimizes overall operation, which subsequently enables potential weight reduction benefits.

Figure 5 presents a high-level view of the control system and interactions of the subsystems; more detail is provided on the individual subsystems in the following sections. The upper left corner contains the flight control block, the rest of the figure depicts the powertrain control. The flight control block accepts pilot and autopilot inputs, and allocates commands to the flight control effectors, comprising the flight control surfaces and the EEs. The use of EEs to augment the flight control surfaces creates an integrated flight and propulsion control (IFPC) system. Some earlier approaches to IFPC developed for traditional aircraft considered the propulsion system to be a flight control actuator (e.g., Refs. 4 and 5) at the bottom of a hierarchical structure. Here the IFPC task is one of several functions of the complex powertrain control system, whose actions are coordinated, and to some extent supervised (Ref. 6), within the context of the powertrain operation.

SUSAN's powertrain encompasses the power-producing and thrust-producing components, and all components in between. The boxed area in Figure 5 provides a representation of its overarching control system. The throttle (or autothrottle) command enters at the lower left and is mapped to a speed command for both the GTE and EEs. It should be noted that the speeds are determined such that the resulting thrust split of 1/3 from the GTE, 2/3 from the EEs is maintained; the GTE is designed to accommodate the power extraction necessary to achieve EE speed in steady state around the flight envelope. Since there is only a small amount of variation allowed in the power extracted from the GTE for it to maintain acceptable operation, it implies that the speed commands are coupled. The speed commands are nominal setpoints to the GTE control system (bottom right of the figure) and each EE control system (top right of the figure). The setpoints can be modified based on specific needs and situations, as indicated by the adjustment from the flight control block. The commands for differential thrust to aid in maneuvering helps limit the movement and potentially the size and weight of the flight control surfaces. These commands are implemented symmetrically such that speed increases on one side are offset by speed

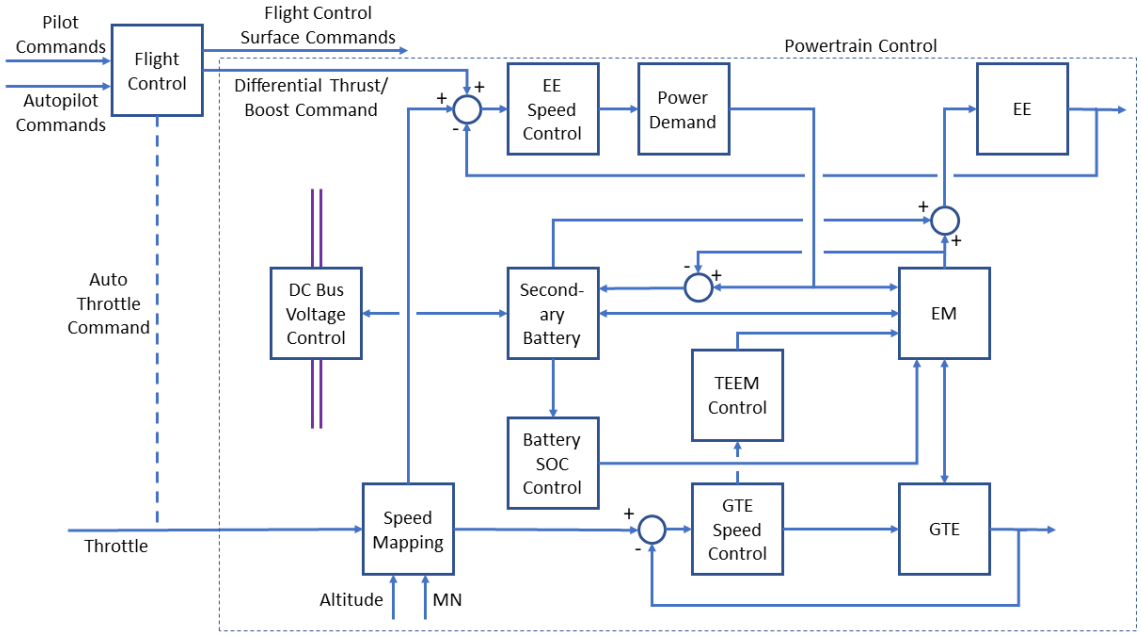

Figure 5.—SUSAN control structure emphasizing the elements of the powertrain control. For simplicity, components of which there are multiple copies, such as EEs, EMs, and batteries, are depicted only once.

decreases on the opposite side, resulting in essentially no change in power requirement. Boost, on the other hand, requires all EEs to increase in speed to provide additional thrust during part of the climb phase. Currently, boost is envisioned as an augmentation of 2 MW for 5 min at top of climb. In this case, the GTE cannot accommodate the additional power extraction, so the secondary batteries must supply the shortfall (which drives their sizing requirement). This is indicated in the middle of the figure by the difference between the power demand and the EM output being sent to the battery, whose output is added to that of the EM to power the EEs.

Directly above the GTE Speed Control Block, at the bottom right of the figure, is the TEEM (Turbine Electrified Energy Management) Control block. This algorithm is initiated when there is a significant difference between the GTE setpoint and the measured value, indicating the GTE is undergoing transient aerodynamic loading affecting operability. TEEM utilizes the EMs to momentarily add or extract mechanical power from the LPS and HPS to obtain improvements in GTE operability. Engine operability places constraints on engine design that sacrifice transient performance, so TEEM provides the potential to reduce the size and weight of the GTE. The TEEM algorithm requires an energy storage element to resolve electrical energy imbalances encountered during transients. The secondary battery provides this independent energy source to facilitate TEEM. Boost and improved acceleration of the EEs are also accommodated by the secondary batteries, as well as DC bus voltage regulation through a controller shown to the left of the battery in the figure). The battery state of charge (SOC) is managed through use of the EMs.

There is also some higher-level supervisory logic required in specific situations, which is not shown in Figure 5. Initiation of boost is an example where awareness of the aircraft state with respect to the flight plan is required, which can be incorporated into the autopilot. With boost as well as with TEEM, the battery must be allowed to discharge below its setpoint without its SOC controller acting to restore it. This condition occurs because the power extraction from the GTE is not sufficient to accomplish these tasks, so battery power is required. Once the action is complete, the battery recharges over time by demanding a small amount of additional power extraction from the GTE.

Trade studies will determine which components to use as well as their size, weight, and location, but these decisions should not fundamentally change the control concept.

Turbine Engine Control

The SUSAN GTE is structured like the Advanced Geared Turbofan 30K (AGTF30) (Figure 6), with a similar control system (Ref. 7). The installed design incorporates Boundary Layer Ingestion (BLI). The two-spool engine has a geared fan attached to the low-pressure shaft. The control system has a standard Proportional-Integral (PI) min-max form with fan speed control. The max limits include: Wf/Ps3, T45, Nf, N2, and Ps3. The min limits include: Wf/Ps3 and Ps3. There are two additional actuators, the Variable Bleed Valve (VBV) and Variable Area Fan Nozzle (VAFN). Both VAFN and VBV are scheduled on corrected fan speed (Nfc) and Mach Number (MN) within the operational envelope. The VBV maintains the stall margin above 10 percent. The VAFN produces optimal fan performance at all operating points by maintaining a specific pressure ratio (PR) given a corrected flow (Wc) and Nfc.

The engine is designed for a large amount of power extraction through EMs attached to the HPS and LPS. However, although the amount of power extraction is large, the variation at any point is relatively small. This potentially has implications when a generator or EE fails, as limiting the powertrain's ability to consume power generated by the GTE directly impacts the GTE's operability and thus could force a reduction in thrust setting.

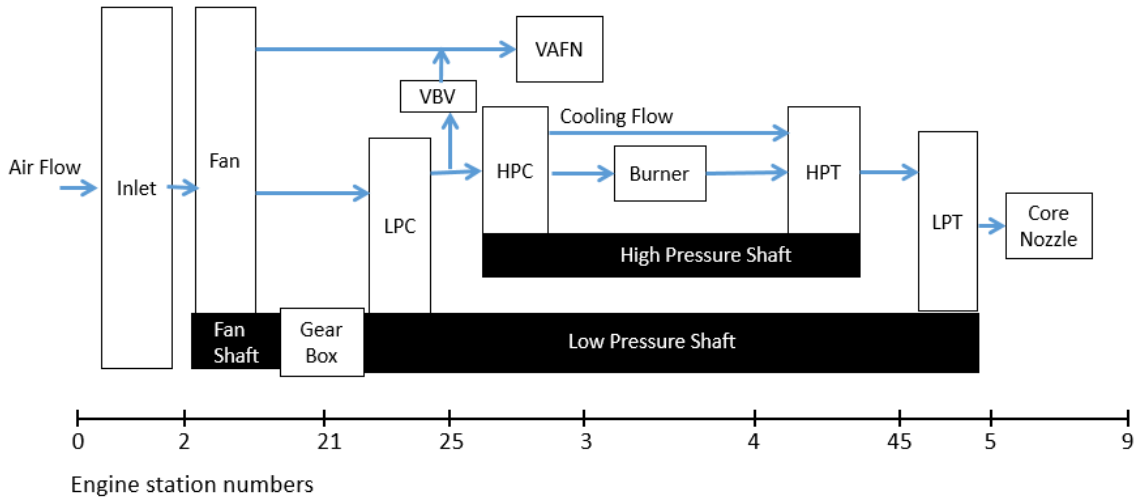

Figure 6.—Diagram of the AGTF30, which has a structure similar to that of the SUSAN GTE, showing station numbers.

TEEM Control

The TEEM control (Refs. 8 and 9) uses EMs, i.e., motors/generators, attached to the high- and low-pressure shafts of the engine as additional actuators available to the control system. Figure 7 is a schematic of the high-level control system architecture. The TEEM portion is implemented through the electric machine torque controllers and TEEM activation/deactivation logic. Because TEEM may source or sink power during transients, logic is present for charging/discharging the energy storage system back to its desired SOC.

During transient operation, the EMs add or extract power from the shafts as appropriate to coordinate the acceleration or deceleration of the spools with the flow state within the engine. The approach is to coordinate the shaft speeds of the engine with the commanded fuel flow rate via a schedule that corresponds to the steady-state operating line of the engine. Perfectly executed without constraints, TEEM would keep the turbomachinery components operating on their steady-state operating lines through the duration of transients. In practice, limitation on EM power, modifications to the control approach due to EM effectiveness, and elements of uncertainty/variation will prevent an ideal result. However, the idea remains the same and the impact remains significant. Use of the EMs during transients will suppress excursions from the transient running line toward the stall line as depicted in Figure 8 when compared with a traditional turbine engine control system. The reduction in transient operability stack normally designed into compressors can be leveraged in the engine design process to increase efficiency and reduce weight.

The TEEM control strategy employed in SUSAN is very similar to what is described in References 8 and 9. A dual-spool TEEM approach is utilized given that EMs are present on both spools. While the approach in References 8 and 9 only injects power onto the HPS during accelerations, in this application power is injected onto both spools using shaft speed control as the means of determining the EM torque commands. The benefit in this application is to keep the engine spool speeds more in sync, thus preventing excessive HPS speed overshoot. This approach was demonstrated in a different application described in Reference 10. During decelerations, the LPS EM is commanded to achieve the desired LPS

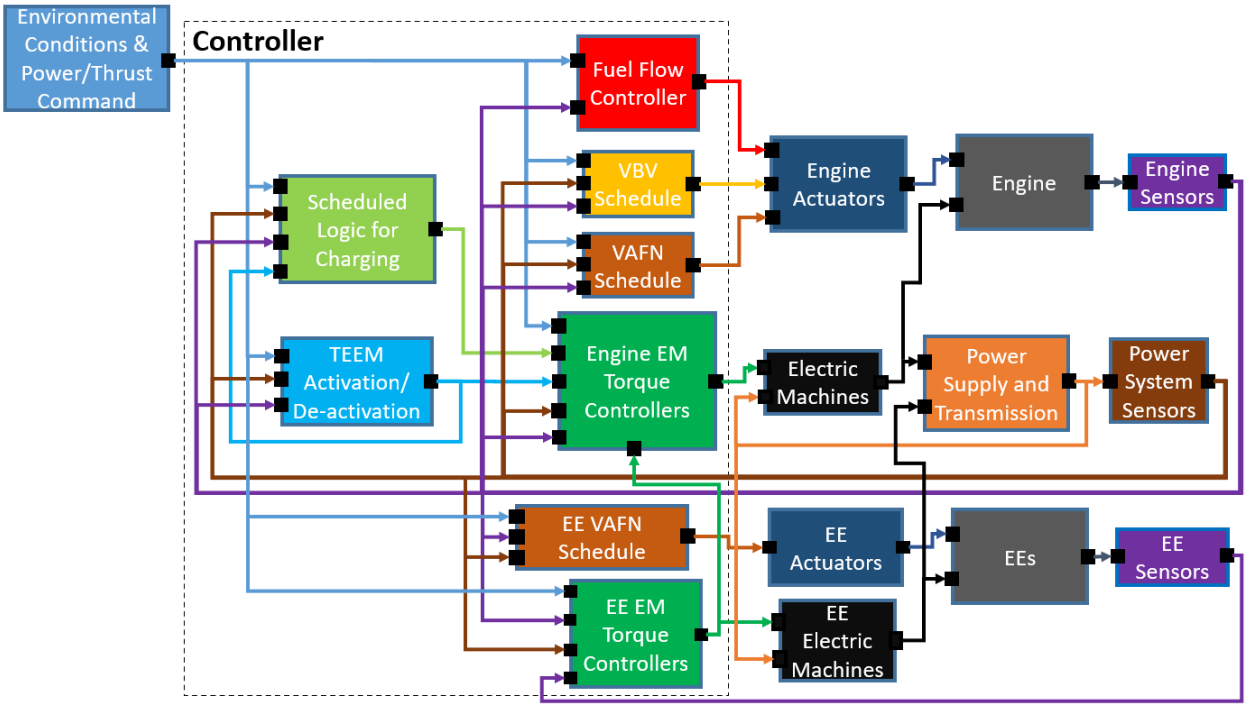

Figure 7.—High level representation of the overall control structure.

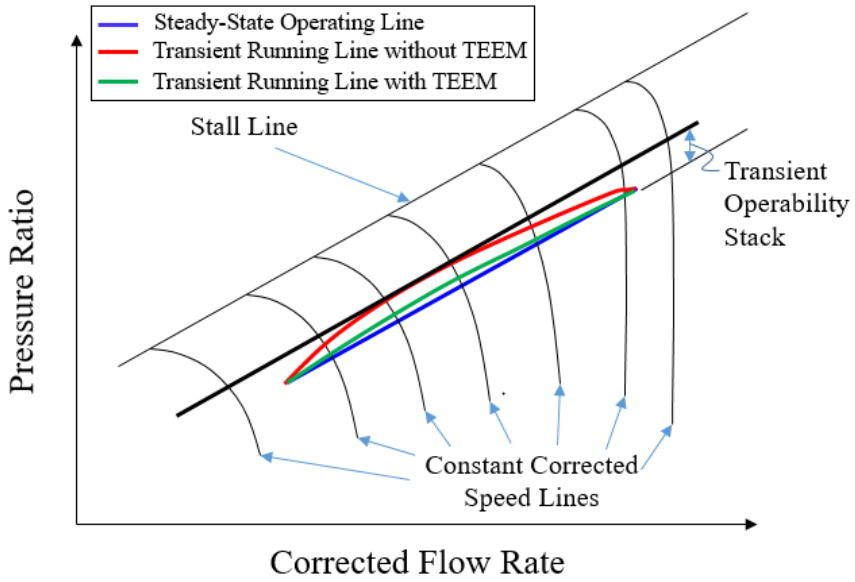

Figure 8.—Illustration of TEEM impact on a compressor map.

speed while the HPS EM is commanded to inject any power extracted from the LPS to the HPS. The power transfer to the HPS tends to further boost the LPC operability that is of concern during decelerations, and it resolves the issue of what to do with excess power extracted from the LPS. The TEEM torque commands are limited to reduce power usage from the EMs, thus potentially reducing the size of the secondary batteries. The control strategy described above is taken from the perspective of the engine and its shafts. Another way to look at it is from the perspective of the power system that employs TEEM. Rather than treating power extraction/insertion as the control input, the control inputs distill down

to the throttling inverter current demands necessary to supply the torques needed to influence the shafts. The energy storage system has no knowledge of what the engine is doing, only concerning itself with voltage regulation, filling in the voids or absorbing the excess energy as needed.

Transient detection logic is used to determine if a transient is occurring, and this information is used to activate or deactivate the TEEM controller. Again, the approach utilized in References 8 and 9 is applied. This entails computing a normalized error of the setpoint of the active min-max controller and comparing it to a threshold value. If the magnitude of the normalized error is below the threshold, steady-state operation is assumed. Otherwise, if the normalized error is greater than the threshold and positive, acceleration is indicated, and if the normalized error is greater than the threshold and negative, deceleration is indicated. The logic is important to assure that off-nominal torques are not applied to the shafts during steady-state operation, which could result in shifts in performance and non-zero net power. The normalized error metric is also used to aid with transitioning from an active TEEM controller to a nonactive TEEM controller. To encourage a graceful transition of the TEEM controller, the TEEM torque commands are multiplied by a taper factor between 0 and 1 defined by a logistic function of the normalized error. As the error approaches zero, the taper factor will begin to approach zero, thus reducing the TEEM torque commands.

Given the usage of power from batteries when implementing TEEM, the secondary batteries need the ability to recharge in flight to minimize their size. Thus, a SOC controller is included to command additional power extraction or insertion from the EMs. Additional power is taken off the LPS and additional power insertion, if applicable, is put onto the HPS. These actions tend to improve compressor operability. The dynamics of the SOC controller are much slower than the TEEM controller, and the commanded powers are limited such that the SOC controller will not counteract the TEEM controller. Limiting the SOC power commands also limits any shifts in performance.

Power System Control

The power system must deliver the power necessary to operate the EEs and to implement TEEM control, all while regulating the DC bus voltage. In the current configuration, a DC-DC converter between the DC bus and the battery maintains bus voltage as necessary using a PI controller to source power from or sink it to the battery. During steady state operation, the power extracted from the turbine will equal the amount required to drive the EEs. If the power demand is so great that it causes the bus voltage to droop, the temporary shortfall is made up by the batteries through the DC-DC converter. Likewise, if the power demand temporarily drops below the level being extracted from the turbine, the batteries absorb the excess, and their SOC will increase. Once the batteries are fully charged, or if they cannot charge quickly enough and the bus voltage increases, the excess power is dumped, preferably in a useful way such as through an anti-icing system. The batteries themselves use a PI controller to maintain their SOC by sending an incremental torque command to the EMs.

The EMs in the system comprise the four main generators on the LPS, the motor/generator on the HPS, and the two motors for each of the 16 EEs.[3] The EMs themselves respond to a torque command through PI control. As mentioned previously, the TEEM control modifies the torque command to the EMs on the GTE shafts. When the EMs are operated under speed control, the command to the torque control is modified by an outer loop PI controller responding to the speed error.

[3]It is possible that the EE EMs could be used for power generation for battery charging during descent.

Electric Engine Control

In the current version of SUSAN, there are eight EEs in a mail slot nacelle mounted under each wing (see Figure 1). Each EE has variable speed contrarotating fans (Figure 9). Thus, the speed of each EE is maintained by adjusting the torque on its fan shafts. Because each EE has two fans on a common axis, there are two motors, each with its own controller. A PI controller is used to ensure the desired speed is achieved by requesting torque from the motors, as shown in Figure 10. In the current design, each EE also has a scheduled VAFN, although this feature is not expected to be retained as the mail slot design matures.

Under normal operation (without differential thrust), the EE speed setpoint is scheduled based on engine corrected fan speed, altitude, and Mach number. The objective is to keep the EEs coordinated with the GTE. This means that not only are the GTE fan and EE speeds related, but that the power extraction and consumption are equal. The EEs demand power from the EMs connected to the GTE. The SOC controller modifies that command as necessary to ensure that the batteries reach their setpoint. During steady-state operation with adequately charged energy storage, the SOC controller ensures all the power extracted from the engine is consumed by the EEs. This trade-off of information between the GTE and EEs helps to keep them coordinated.

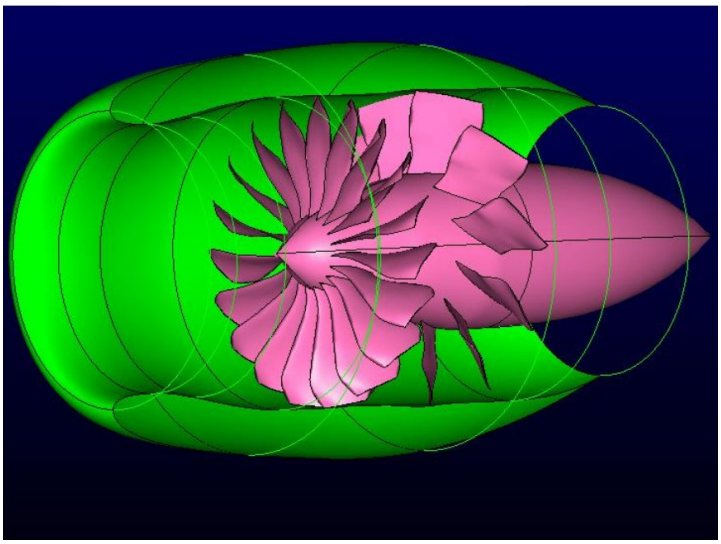

Figure 9.—Contrarotating electric fans.

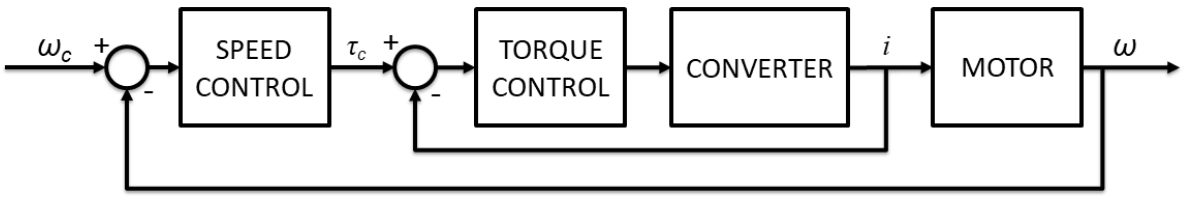

Figure 10.—Outer Loop Speed Control with Inner Loop Motor Control. The speed control demands a torque, τ_c, the torque control demands a current, i.

Powertrain Supervisory Control

The Powertrain Supervisory Control helps coordinate the power and propulsion systems, and it has several important functions. These tend to be generally above the functional level shown in Figure 5.

Power Boost

Under certain conditions, for instance near top of climb, the usual thrust split (1/3 from the GTE, 2/3 from the EEs) is not adhered to. In this case the GTE still supplies the power for the EEs to produce twice the GTE's thrust, but the batteries augment the power. This way the EEs achieve an even higher thrust level. This allows the turbofan engine to be smaller and lighter than it would be if it needed to provide all the power itself. The supervisory control needs to ensure that overall, there is sufficient power available for the desired action. As mentioned in the Control System Overview section above, boost initiation could be incorporated into the autopilot.

Monitor Battery State of Charge

The supervisory control, in conjunction with the Battery Management System (BMS), monitors the battery SOC, ensuring that there is capacity to accept excess power and power available to meet any needs of the powertrain. When the battery SOC is out of its nominal range, the supervisory control coordinates the powertrain behavior to recover the nominal state while maintaining thrust. If the demands of normal operation cannot be met given the current battery SOC, the supervisory control replans the operation accounting for the current battery status.

Figure 11 shows an example battery discharge curve in terms of voltage as a function of SOC. The usable battery operating voltage range (between V_{max} and V_{min}) is essentially constant, while the SOC range from Q_{max} to Q_{min} is quite large. The battery SOC should remain constant during normal operation, with the power extracted from the GTE being fully consumed by the EEs. However, the nominal SOC value allows for some excess power absorption, as well as power dissipation, for multiple reasons. These include boost, TEEM, and rapid acceleration of the EEs.[4] The SOC controller adjusts the power extraction when SOC is to be maintained. However, when battery power is required, the SOC is allowed to drop. The battery is sized such that the nominal SOC range should be sufficient for all situations. However, battery charge and discharge rate limits may impact operation in some cases.

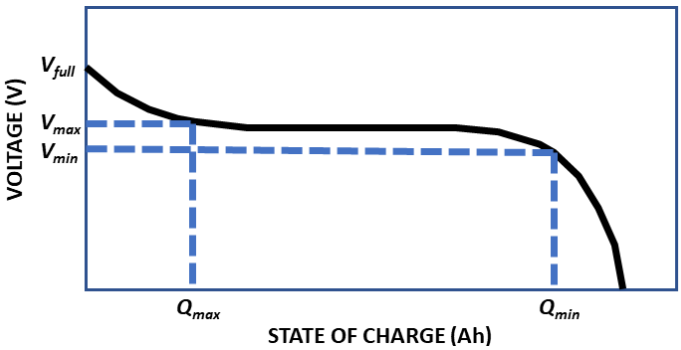

Figure 11.—Battery Discharge Curve.

[4]When the throttle position is increased quickly, the turbine engine takes several seconds to respond, but the EEs are expected to accelerate much more quickly. While the turbine response is lagging the EEs, it cannot provide the additional power they require, so the secondary batteries fill in the power deficit as the GTE spools up.

Coordination with BMS and IVHM system

The BMS is an electronic system that monitors and manages the battery to keep it within its safety margins. The BMS is responsible for monitoring the battery SOC, state-of-health (SOH), state-of-power (SOP), and remaining useful life (Refs. 11 and 12). The BMS can also perform thermal management and cell balancing, and ensures the battery does not overcharge or over-discharge, which affects safety and can shorten the battery life (Ref. 13).

The powertrain Integrated Vehicle Health Management (IVHM) system will support the Supervisory Control to implement appropriate reversionary control modes such as those that involve TEEM (Ref. 10). Previously mentioned control functions may be impacted by faults, battery rate limits, etc., and these changes must be accounted for.

Integrated Vehicle Health Management

An IVHM system requires a multidisciplinary approach that enables automatic detection, diagnosis, prognosis, and mitigation of adverse events arising from component failures (Ref. 14). In the context of the SUSAN powertrain, the IVHM system monitors the GTE, the power system, and the EEs. In addition, the airframe might have structural health monitoring, sensor and actuator health monitoring, etc. The IVHM system detects, isolates, and can help accommodate faults. It provides prognostic information that supports mission modification, if necessary. Along with the BMS, flight control, and powertrain supervisory control, the IVHM system supports redistribution of power to EEs in case of specific motor failures, and control reconfiguration in general. With SUSAN it is anticipated that a vast array of potential powertrain faults will be handled automatically up to the limits of the system. The built-in redundancy allows EE and potentially even a generator failure to be accommodated without significant performance impact, and a GTE failure is mitigated using the primary batteries, although this is an emergency situation. While IVHM is not the focus of this paper, it is important to note that most of the mitigation strategies are expected to be control-enabled.

Flight Control

The SUSAN Flight Control System (FCS) uses a three-loop baseline controller similar to the structure found in Reference 15. This structure is modified to handle the complexities arising from the number of EEs and integration between the flight, propulsion, and power system controllers. The three loops are: autopilot, outer loop, and inner loop as shown in Figure 12. The baseline controller achieves the performance requirements of the vehicle with cascaded Proportional-Integral-Derivative (PID) feedback controllers augmented with feed forward terms, as described in the following subsection. The baseline controller is modified to include control allocation and propulsion compensation methods to integrate the

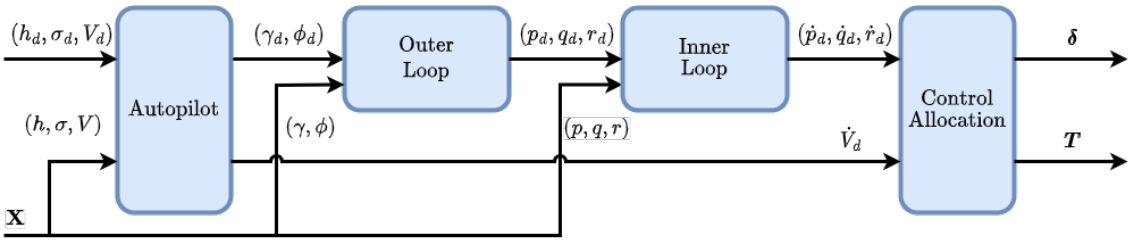

Figure 12.—Flight control architecture.

baseline controller with the Distributed Electric Propulsion (DEP) system. The control allocation algorithm handles the large number of propulsors and can be used to implement differential thrust commands. The propulsion compensation method informs the power distribution system of the desired power to improve vehicle performance. These modifications are described in the subsection after next.

Baseline

The baseline controller regulates the vehicle altitude, course angle, velocity, orientation, and body rates based on feedback from the vehicle state.

The autopilot regulates the altitude, course angle, and airspeed of the vehicle with PID controllers designed to track the desired values, indicated with a subscript, d, provided by a mission planner. Based on the tracking error and current airspeed, the altitude controller produces a desired flight path angle, γ_d. Similarly, the course angle autopilot is a PID controller that produces the desired roll angle, ϕ_d, based on the course error and airspeed. The airspeed controller tracks a calibrated airspeed target by commanding acceleration with feed forward flight path angle compensation.

The outer loop controller uses a PID controller to generate body frame rate targets, p_d and q_d, based on tracking error of the roll and flight path angles respectively. The body rate target, r_d, is chosen based on a coordinated turn constraint computed from measurements of inertial velocity, angle of attack, sideslip angle, and roll angle.

The inner loop controller uses PID control to produce desired body frame rotational accelerations to reduce errors in the body frame rotation rates. These desired accelerations are sent to the control allocation system for conversion into desired control surface deflections, and when under autopilot control, autothrottle commands (thrusts) (see Figure 12).

Integrated Flight and Propulsion Control

The flight control incorporates DEP for enhanced maneuvering. This has the potential to allow reduction in the size of the rudder, providing a weight savings. The concept is that for turning, the EEs on one side speed up while those opposite slow down, providing a turning moment while maintaining total power draw. This way the thrust differential augments the rudder effectiveness, while the ailerons counteract the induced roll. Note that if DEP is designed into the flight control system, differential thrust (speed) commands to the EEs will enhance rudder commands even when hand flying. The output of the baseline flight controller is given in terms of desired linear and rotational accelerations. Control allocation converts these accelerations into commands for each of the individual control effectors. Due to the large number of effectors, a weighted pseudo-inverse allocation is implemented, as described in Reference 16. This allocation method directly computes the mapping from accelerations to effector inputs based on the inverse of the linearized control effectiveness matrix of the vehicle. Furthermore, the produced mapping will reduce cross-coupling between control axes, if possible. The weighting function of the algorithm allows the designer to reduce or remove the contribution of specific effectors.

In autopilot mode, the flight control system sends a desired thrust command to the propulsion system. The propulsion system divides this desired thrust between the GTE and EEs as steady state RPM targets. However, the EEs' response rate is limited by the amount of power available for use. To preempt the demand for power from the EEs, the flight controller also sends the desired thrust to the engine control system as a dynamic feed-forward term. The feed-forward term improves the response rate of the propulsion system whenever thrust targets are changed, such as accelerating into a climb maneuver.

Discussion

The various subsystems and the envisioned control schemes for the SUSAN concept were described in the previous sections. The interaction of the subsystems and resulting complexity of the control system, when taken as a whole, significantly exceeds that of current commercial airliners with independent flight and propulsion control systems, and individually controlled engines. The complexity of the SUSAN design is expected to bring with it new ways to optimize the vehicle. Margins can be reduced in multiple instances as control-enabled benefits are realized. The boost capability means that the engine can potentially be sized for closer to cruise, where it spends most of its time in the air. TEEM control can potentially reduce the engine size further, while DEP-enhanced maneuverability can reduce the size and weight of flight control surfaces. Ultimately trade studies will demonstrate if these benefits can be fully achieved, since batteries and related components must be added, and in some cases future technological improvements are anticipated based on current trends. However, the control development that is going into the concept is enabling, and is, therefore, required in parallel with component hardware research.

Significant progress has been made on the creation of a dynamic model of the vehicle and powertrain (Ref. 17) as well as on the development of the control system described here. This type of integration, in a simulation model, helps to validate the control concept and expose shortcomings. While it does not directly prove the weight savings, it does demonstrate the control benefits that could enable them. Figure 13 displays plots of a burst and chop transient, one in which the Power Lever Angle (PLA) is moved rapidly from a low to high power setting, then after allowing time to settle, moved rapidly back to the original setting. Here TEEM control is active during the acceleration and deceleration transients. The battery SOC reduces during the acceleration as torque is applied to both shafts, recovers once TEEM control is complete, and increases slightly during the deceleration, returning to baseline once the transient is complete. It is clear that the torque required for TEEM is small compared to the power extracted from the LPS for the EEs. Here the EEs accelerate and decelerate along with the GTE, i.e., rapid response has not yet been implemented. Even with this feature not yet incorporated, the figure gives an idea of how the subsystems interact and work together to deliver the required performance.

Figure 14 shows a coordinated turn where the rudder function is assigned to the EEs. Here the EEs provide the desired turning moment and a resulting rolling moment. The thrust is spread across the wings such that increases on one side are compensated by decreases on the other side, with the outermost (most effective) EEs changing the most. Comparing the top (ailerons), fourth (roll angle) and bottom (EE thrust) plots in Figure 14, it is clear how the ailerons manage the bank angle and compensate for the disturbances induced by the EEs. Figure 15 shows an enlarged annotated version of the EE thrust plot from Figure 14. It shows how the flight control modifies the EE thrust throughout the turn.

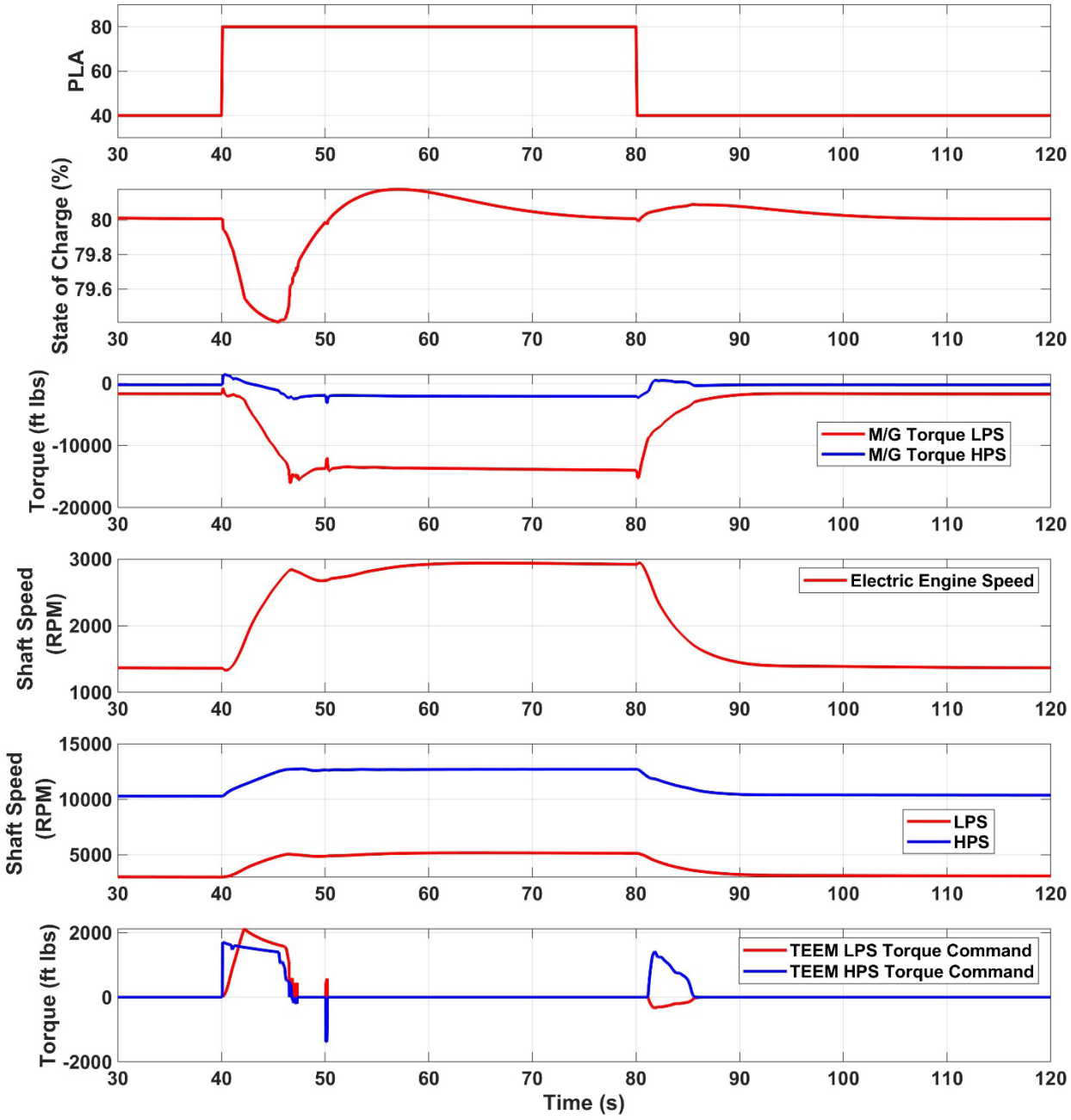

Figure 13.—Burst and Chop transient. The top plot shows the power command. The second plot shows the battery SOC throughout the transient. The third plot shows the total torque on both the LPS and HPS. The fourth plot shows the EE speed. The fifth plot shows the LPS and HPS speed. The last plot shows the torque command due to the TEEM control, the result of which is visible in the third plot.

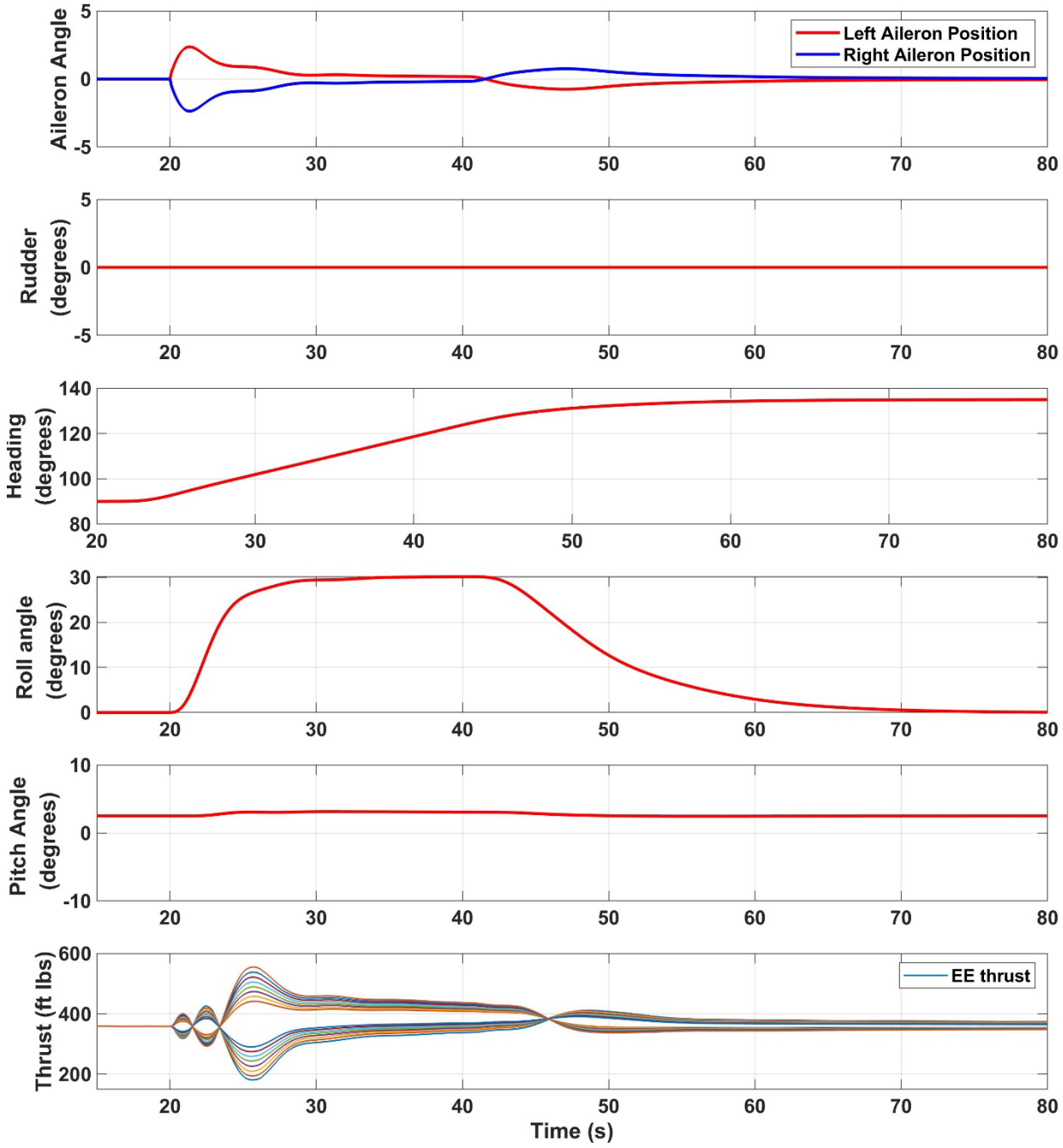

Figure 14.—Coordinated turn using EEs instead of rudder. The ailerons manage the 30-degree bank, accounting for the roll induced by the EEs. The bottom plot shows the EE thrust distribution across the wings, where that of the outermost EEs varies the most.

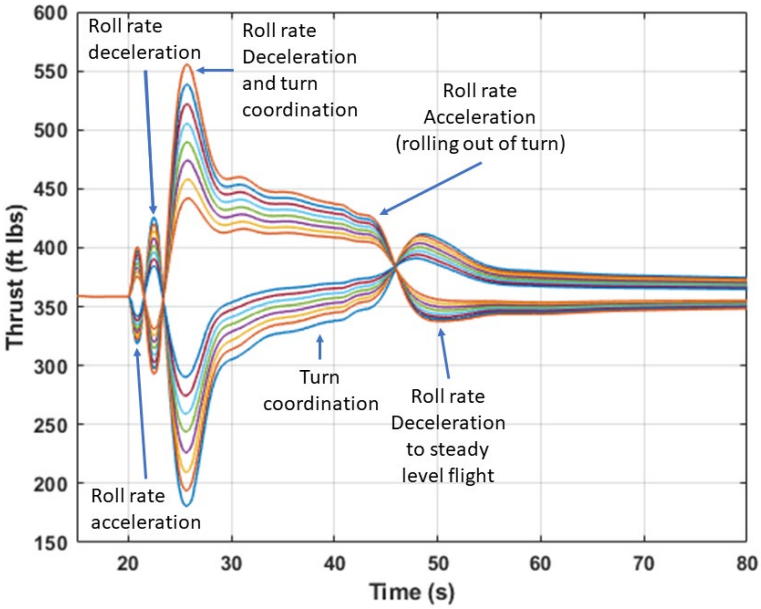

Figure 15.—Annotated plot of EE thrust during a coordinated turn.

Summary

The proposed control approach for the SUSAN concept aircraft was presented. While many of the control concepts described are individually simple, the overall scheme to coordinate the various subsystems is relatively complex. Furthermore, this under-the-hood operation necessarily simplifies the pilot interface with respect to the number of engines because they cannot be independently controlled by the pilot. This is anticipated to be especially true in the case of failures within the powertrain where automatic recovery will be required whenever possible, and pilot intervention will likely be limited to extreme cases, such as diagnosing a malfunctioning GTE. Some of the control functionality has been successfully demonstrated on a preliminary full envelope nonlinear dynamic model. The model has been used to demonstrate TEEM control and DEP-enhanced turning. Both techniques have the potential to reduce aircraft weight. Updates to the model based on the results of future trade studies are not expected to impact the control approach significantly. The restrictions on pilot interaction with the powertrain and the coordination of the subsystems necessary to achieve the required performance imply that the vehicle must be very highly automated. It is, in fact, this very automation that enables much of the projected benefit that the SUSAN concept hopes to deliver.

References

1. Jansen, R.H., et al., “Subsonic Single Aft Engine (SUSAN) Transport Aircraft Concept and Trade Space Exploration,” AIAA 2022-2179, *AIAA SciTech Forum*, San Diego, CA, and virtual, 3–7 January 2022.
2. Haglage, J.M., Dever, T.P., Jansen, R.H., and Lewis, M.A., “Electrical System Trade Study for SUSAN Electrofan Concept Vehicle,” AIAA 2022-2183, *AIAA SciTech Forum*, San Diego, CA & virtual, 3–7 January 2022.
3. Arthur, III, J.J., Kennedy. K., Etherington, T.J., Sachs-Wetstone, J.J., Litt, J.S., and Owen, A.K., “Flightcrew Thrust Control and Engine Display Concepts for the SUbsonic Single Aft ENgine (SUSAN) Transport Aircraft,” *AIAA SciTech Forum*, National Harbor, MD, 23–27 January 2023.

4. Garg, S., “Controller Partitioning for Integrated Flight/Propulsion Control Implementation,” NASA TM-105804, 1992.
5. Fuller, J.W., “Integrated Flight and Propulsion Control for Loss-of Control Prevention,” AIAA 2012-4896, *AIAA Guidance, Navigation, and Control Conference*, Minneapolis, MN 13–16 August 2012.
6. Simon, D.L., “System-Level Control Concepts for Electrified Aircraft Propulsion Systems,” NASA/TM-20210026284, 2022.
7. Chapman, J.W., Litt, J.S., “Control Design for an Advanced Geared Turbofan Engine,” AIAA-2017-4820, *Propulsion and Energy Forum*, Atlanta, GA, 10–12 June 2017.
8. Culley, D., Kratz, J., and Thomas, G., “Turbine Electrified Energy Management (TEEM) For Enabling More Efficient Engine Designs,” AIAA 2018-4798, *AIAA Joint Propulsion Conference*, Cincinnati, OH, 9–11 July 2018.
9. Kratz, J.L. Culley, D.E., and Thomas, G.L., “A Control Strategy for Turbine Electrified Energy Management,” AIAA Paper 2019–4499, *AIAA Propulsion and Energy Forum*, Indianapolis, IN, 19–22 August 2019.
10. Kratz, J.L. and Simon, D.L. “Failure Modes and Mitigation Strategies for a Turboelectric Aircraft Concept with Turbine Electrified Energy Management,” AIAA 2022-1191, *AIAA SciTech Forum*, San Diego, CA, 3-7 January 2022.
11. Ali, M.U., Zafar, A., Nengroo, S.H., Hussain, S., Junaid Alvi, M.J., and Kim, H.-J., 2019, “Towards a Smarter Battery Management System for Electric Vehicle Applications: A Critical Review of Lithium-Ion Battery State of Charge Estimation,” *Energies*, Vol. 12, No. 3, 2019, p. 446.
12. Duan, J., Tang, X., Dai, H., Yang, Y., Wu, W., Wei, X., and Huang, Y., “Building Safe Lithium-Ion Batteries for Electric Vehicles: A Review,” Electrochemical Energy Reviews, Vol. 3, No.1, 2020, pp. 1–42.
13. Ahmed, R., Gazzarri, J., Onori, S., Habibi, S. et al., “Model-Based Parameter Identification of Healthy and Aged Li-ion Batteries for Electric Vehicle Applications,” SAE International Journal of Alternative Powertrains, Vol. 4, No. 2, 2015, pp. 233–247.
14. Integrated Vehicle Health Management of a Transport Aircraft Landing System, white paper, http://www.infosys.com/engineering-services/white-papers/documents/aircraft-landing-gear-system.pdf
15. Yechout, T.R., Morris, S.L., Bossert, D.E., Hallgren, W.F., and Hall, J.K., *Introduction to Aircraft Flight Mechanics*, American Institute of Aeronautics and Astronautics, Reston, VA, 2014.
16. Sadien, E., Roos, C., Birouche, A., Carton, M., Grimault, C., Romana, L., and Basset, M., “A detailed comparison of control allocation techniques on a realistic on-ground aircraft benchmark,” *American Control Conference*, Philadelphia, PA, 2019, pp. 2891–2896.
17. Litt, J.S., Sowers, T.S., Buescher, H.E., Sachs-Wetstone, J.J., Listgarten, N.L., Jansen, R.H., “Implementation Approach for an Electrified Aircraft Concept Vehicle in a Research Flight Simulator,” AIAA 2022-2306, *SciTech Forum*, San Diego, CA, and virtual, 3–7 January 2022.